Hindawi
Journal of Nanomaterials
Volume 2022, Article ID 2284806, 7 pages
https://doi.org/10.1155/2022/2284806

Research Article

Research on Airflow Cooling Characteristics of Titanium Alloy Engine Blade Surface Machining

Lei Qiu,[1] **Shaoyong Zheng**,[2] **Lanlan Liu**,[3] **Shuli Hong**,[1] **and Jun Chi**[1]

[1]*School of Mechanical Engineering, Ningbo University of Technology, Ningbo Zhejiang, China*
[2]*Zhejiang People Industry Facilities Co., Ltd, Hangzhou Zhejiang, China*
[3]*Department of Mechanical Engineering, JiangXi Technical College of Manufacturing, Nanchang, Jiangxi, China*

Correspondence should be addressed to Lei Qiu; qiulei@nbut.edu.cn

Received 25 February 2022; Revised 26 April 2022; Accepted 24 May 2022; Published 10 June 2022

Academic Editor: Awais Ahmed

This paper studied the airflow cooling during blade surface processing and explained the applicable occasions of airflow cooling. The flat heat transfer model was used to study the characteristics of the cooling airflow during blade surface processing. The study of the model showed that the cooling coefficient of the airflow was affected by speed and pressure. Furthermore, the generation and strength of the autogenous cooling airflow were closely related to the physical properties of the grinding tool. In terms of processing heat generation, this paper used the Johnson-Cook material constitutive model to calculate the residual heat on the surface of the processed blade, and the surface temperature rise was within a controllable range. For the airflow intensity generated by the high-speed rotation of the tool, the airflow preset method was used to verify whether it meets the processing conditions.

1. Introduction

Due to the difficult processing of materials [1], the complexity of the shape, the diversity of materials, the diversity of various blade, etc., the difficulty of blade processing has been heavy. The key technologies of blade processing are thorny problems that the aviation industry urgently needs to overcome. Taking compressor blades as an example, they need to be forged or cast billet, milling, surface grinding, and other processes (such as manual polishing of the blade surface and dynamic balance adjustment of the blade) [2, 3] before they can be assembled to the shaft system; Figures 1 and 2 show a milled blade and its surface grinding technology. The machining accuracy of the blade has a great influence on the high-speed rotation accuracy of the shaft system and the performance of the whole machine [4–6]. In recent years, the development of blades with small aspect ratios and curved blades has put forward new requirements for blade processing accuracy and processing methods [7, 8]; the reason for this difficulty is that the geometry of the small aspect ratio blade is more complex than that of the general blade, which is difficult to complete with the existing processing technology. Such blades often need to undergo more complex surface grinding and surface coating layer process treatment. In summary, blade surface processing technology is the core technology of blade production.

Cooling during blade processing is a long-term concern. Due to the heat dissipation of titanium alloys, the surface of the blades will be ablated during the processing, and the local high temperature during the processing of nickel-based alloy blades will change the properties of the blade materials. The form of cooling and the control of cooling conditions are factors that cannot be ignored in blade processing technology.

2. Application of Airflow Cooling and Mathematical Model

There are many cooling methods for surface grinding [9–11]. In the grinding machine processing that uses a high-speed rotating hard grinding wheel as a grinding tool, coolant is usually used for cooling. This cooling method can not only take away the high temperature generated by

Figure 1: Blades formed by CNC milling.

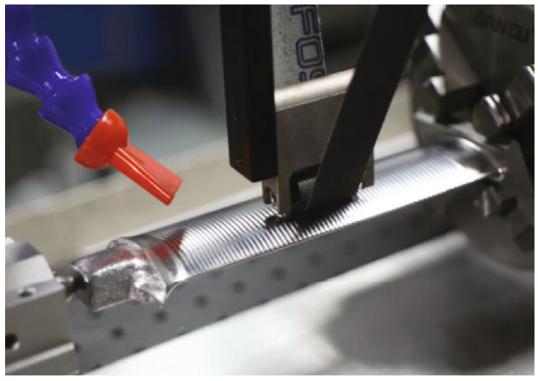

Figure 2: Blade surface grinding technology.

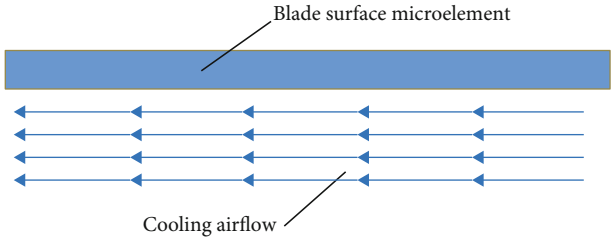

Figure 3: Flat plate heat transfer model.

the processing heat, but it also can wash the surface of the workpiece and the surface of the grinding wheel at the same time and then take away the chips. In the abrasive belt grinding process, since the base material of the abrasive belt is a flexible material, it is not suitable to use a liquid cooling medium, and airflow is often used as a cooling medium. Compared with liquid, airflow cooling does not have particularly high cooling efficiency, but it has several obvious advantages.

First of all, the airflow cooling will not change the properties of the abrasive belt base material, the airflow cannot be attached between the abrasive belt base material and the contact wheel, and the movement form of the abrasive belt will not be changed; secondly, the airflow will not form residues on the surface of the workpiece and will not spread to the gap between the workpiece and the fixture, and the movement

Table 1: Johnson-Cook model parameters for Ti6al4v.

A	B	n	m	T_m	T_r
1098	1092	0.93	1.1	1630	20

Table 2: Parameters for Johnson-Cook model damage.

d1	d2	d3	d4	d5	Tm	Tr	Reference strain rate
-0.09	0.25	0.5	0.014	3.87	1630	20	1

state of the workpiece will not be changed; third, the air flow launching device can be far away from the workpiece, thereby preventing interference in space; fourth, under the same power, the speed of the gas flow is higher than that of the liquid, which helps to increase the circulation frequency of the cooling gas. Obviously, the shortcomings of airflow cooling must be paid attention to and overcome. Due to the Brownian motion of gas molecules, the cooling airflow spreads quickly; therefore, a cooling airflow recovery device must be installed during the grinding process of the blade surface using airflow cooling. Since the recycled airflow is mixed with chips falling off the surface of the blade, abrasive particles dropped due to abrasive belt wear and various metal dusts, the processing environment must be ventilated, smoke and fire are prohibited, and employees must be equipped with breathing system protective masks.

The cooling air flow passes through the surface of the blade being processed and takes away the heat generated by the processing. This physical process can be illustrated by a flat plate heat transfer model. In the model shown in Figure 3, a certain microelement on the surface of the blade is taken as the research object. Since the selected microelement is small enough, its surface can be regarded as a plane approximately. The surface of the microelement is parallel, and the influence of the difference in the direction of the air movement can be corrected on this model. It is worth noting that according to the definition of fluid mechanics, the airflow velocity near the blade is distributed in a gradient, the airflow velocity closer to the blade is slower, and the airflow velocity farther away from the blade is faster. However, in this model, whether the blade or the airflow microelements are small enough that the airflow gradient distribution is very weak, which is ignored for the convenience of calculation.

The temperature distribution under this condition can be analyzed by the method of combining the N-S equation and the energy equation. When the cooling airflow and the processing speed reach a steady state, the governing equations of air flow heat transfer near the blade element should satisfy the following conditions.

Mass conservation equation:

$$\frac{\partial \rho}{\partial t} + \frac{\partial (\rho u_i)}{\partial x_i} = 0. \quad (1)$$

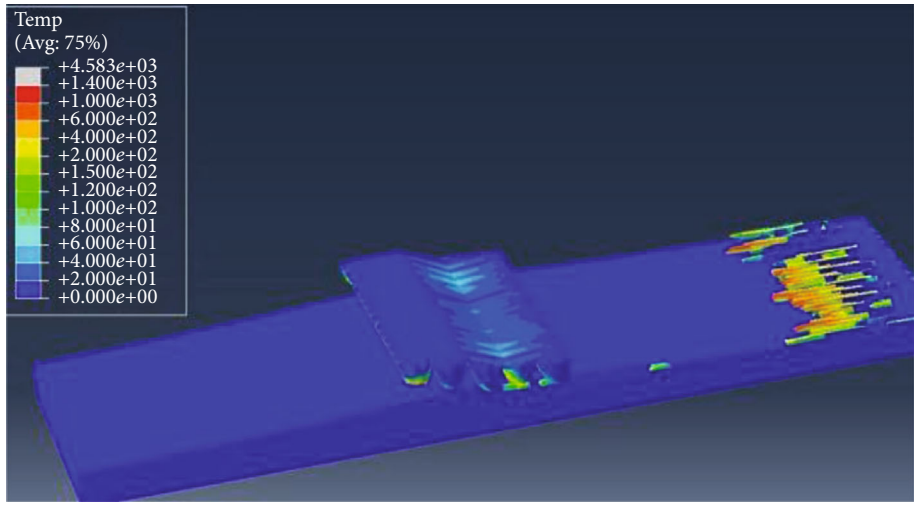

Figure 4: Temperature distribution of the abrasive grain group passing through the highest peak of the blade.

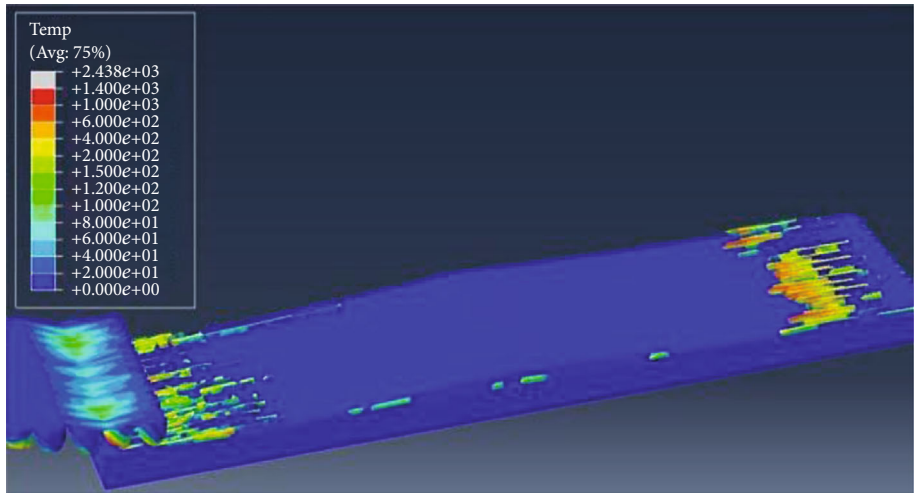

Figure 5: Temperature distribution of the abrasive grain group leaving the blade.

Momentum conservation equation:

$$\frac{\partial(\rho u_i)}{\partial t} + \frac{\partial(\rho u_i u_j)}{\partial x_i} + \frac{\partial p}{\partial x_i} - \frac{\partial \tau_{ij}}{\partial x_j} + \rho g_i + S_i = 0. \quad (2)$$

In the above two formulas, t is the cooling airflow density, p is the airflow pressure, u is the airflow velocity, τ is the viscous stress tensor, and S is the source term of the momentum equation.

The energy conservation equation in the cooling airflow region is

$$\frac{\partial(\rho c_p T)}{\partial t} + \frac{\partial(\rho u_i c_p T)}{\partial(x_i)} - \frac{\partial}{\partial x_i}\left(k_e \frac{\partial T}{\partial x_i}\right) - S_T = 0. \quad (3)$$

The energy conservation equation in the microelement region of the processed blade is

$$\frac{\partial(\rho c_p T)}{\partial t} - \frac{\partial}{\partial x_i}\left(k \frac{\partial T}{\partial x_i}\right) - Q_T = 0. \quad (4)$$

In the above two formulas, c_p is the specific heat capacity, Q_T is the heat source, k_e is the effective thermal conductivity, k is the molecular thermal conductivity, S_T is the source term of the energy equation, and k and k_e satisfy the following relationship:

$$k = k_e - k_r. \quad (5)$$

The definition of k_r is

$$k_r = \frac{c_p \mu_r}{P_r}. \quad (6)$$

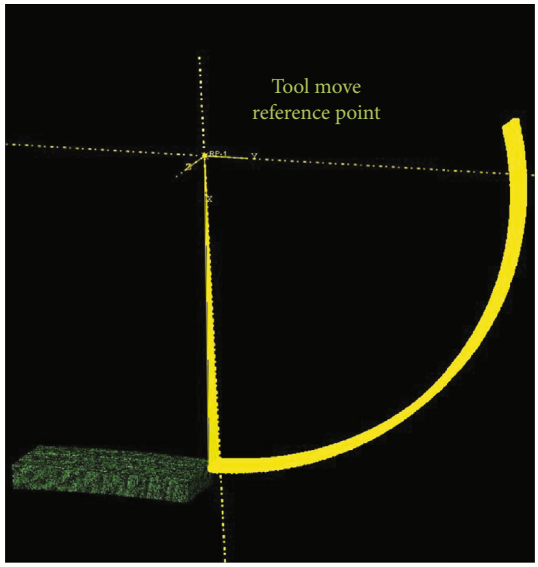

Figure 6: Motion constraint of the stationary state of the blade.

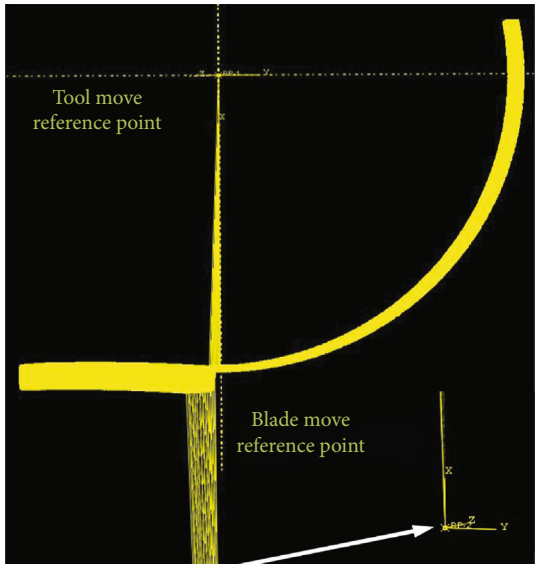

Figure 7: Motion constraints in the case of both blade and abrasive belt movement.

In the above formula, μ_r is the turbulent viscosity coefficient, and P_r is the turbulent Prandtl number.

For the model in Figure 3, the following empirical formula can be used to calculate the heat transfer coefficient:

$$Nu = \frac{\alpha l}{\lambda} = 0.664 R_e^{1/2} P_r^{1/3}. \quad (7)$$

It can be seen from the above formula that the change of the turbulent Prandtl number of the cooling airflow is caused by the change of the turbulent viscosity coefficient, and the change of the Prandtl number causes the change of the plate heat transfer coefficient. However, the heat transfer coefficient is not only affected by the Prandtl number, but also by the airflow Reynolds number. The definition of the turbulent Reynolds number shows that when the speed and pressure of the cooling airflow change, its Reynolds number will change, which will make the blades microelement's heat transfer coefficient changes.

3. Numerical Calculation Model for Processing Temperature

In this paper, the heat generated during the surface grinding of the blade microelement is simulated. The blade material is a new titanium alloy Ti6Al4V.The Johnson-Cook material constitutive model is a thermo-viscoplastic constitutive model suitable for this blade material. The reason for choosing the Johnson-Cook constitutive model is that this constitutive model can not only adapt to the thin-wall shape characteristics of the blade, but also is commonly used in titanium alloys. Research on the dynamic constitutive relationship of metals and mature numerical calculation programs can often achieve better results in grinding mechanism simulation. The mathematical expression of Johnson-Cook material constitutive model is

$$\sigma = (A + B\varepsilon^n)\left[1 + C\left(\ln\frac{\varepsilon}{\varepsilon_0}\right)^m\right]\left[1 - D\left(\frac{T - T_0}{T_0}\right)^k\right]. \quad (8)$$

In the above formula, A, B, n, C, and m are material constants, respectively, representing the yield stress intensity, strain strengthening coefficient, strain strengthening index, strain rate strengthening parameter, and temperature strain rate sensitivity under quasi-static conditions; σ is the flow stress; T_m is the melting point temperature; T is the temperature of the blade material, T_r is the reference temperature, usually designated as the ambient temperature of the simulation experiment; ε is effective plastic strain, and ε_0 is the reference strain rate. The Johnson-Cook material constitutive model parameters of Ti6al4v are shown in Table 1.

In addition to the constitutive model, the simulation of such problems must also define failure criteria. During the grinding process of the blade surface by abrasive particles, the blade material undergoes deformation similar to shear failure under the plowing action of the abrasive particles. Therefore, the failure parameters of the blade material can be defined as follows:

$$\omega = \sum\left(\frac{\Delta\varepsilon^{\mathrm{pl}}}{\varepsilon_{\mathrm{f}}^{\mathrm{pl}}}\right). \quad (9)$$

In the above formula, $\Delta\varepsilon^{\mathrm{pl}}$ is the increase in plastic strain, and $\Delta\varepsilon_{\mathrm{f}}^{\mathrm{pl}}$ is the amount of failure strain.

The failure strain $\Delta\varepsilon_{\mathrm{f}}^{\mathrm{pl}}$ is a function related to the strain rate, compressive stress deviator stress ratio, temperature,

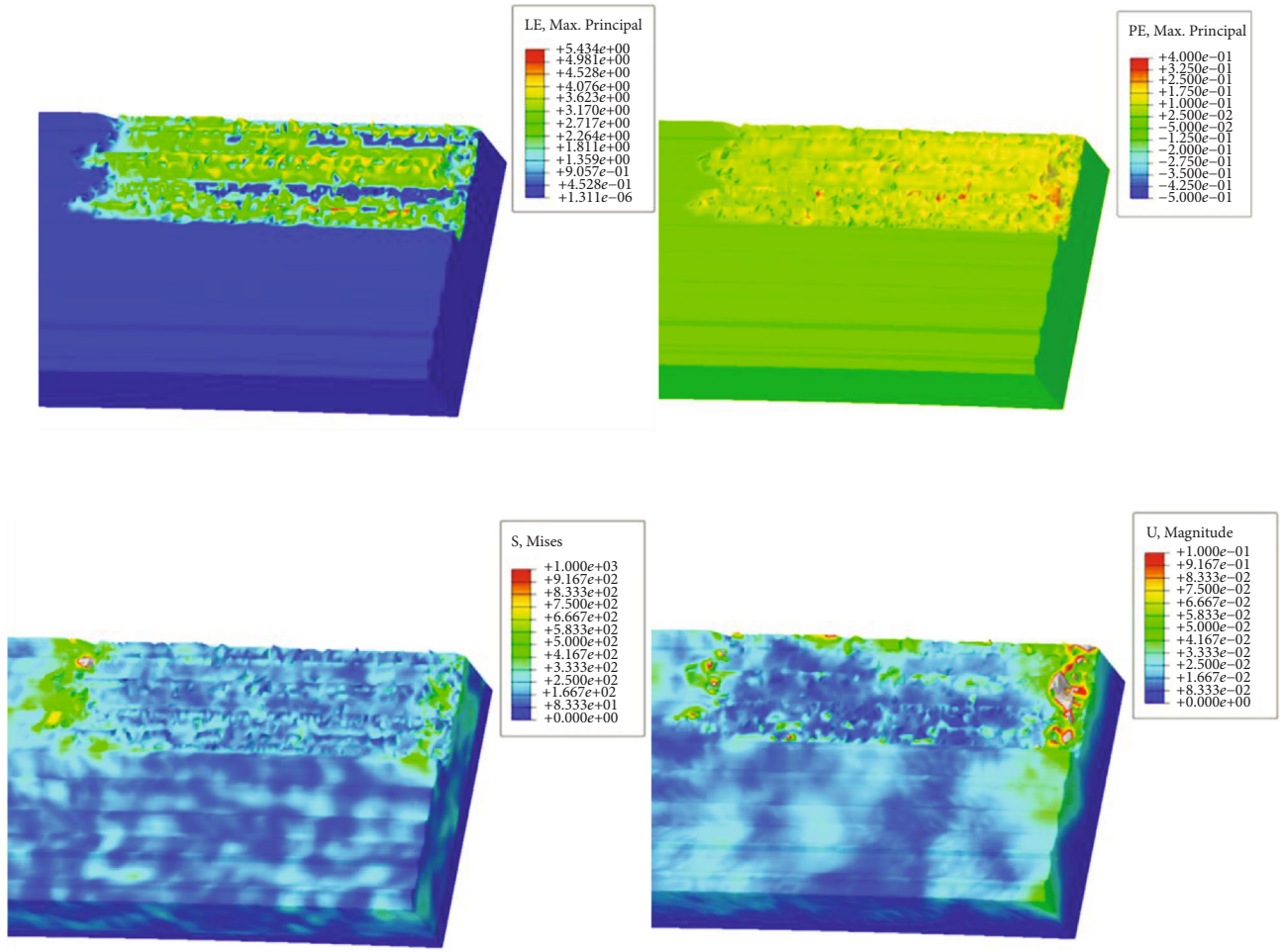

Figure 8: Simulated calculated blade surface with blade feed motion when the abrasive belt is in the initial wear stage.

and other parameters, and its expression is

$$\varepsilon_f^{pl} = \left[d_1 + d_2 e^{(d_3(p/q))}\right]\left[1 + d_4\left(\frac{\dot{\varepsilon}^{pl}}{\dot{\varepsilon}_0}\right)\right](1 + d_3\theta). \quad (10)$$

The dimensionless strain rate in the above formula is denoted as $\varepsilon^{pl\bullet}/\varepsilon_0{}^{\bullet}$, and the compressive stress deviatoric stress ratio is denoted as p/q, where p is the compressive stress and q is the Mises stress. For material Ti6al4v, d1, d2, d3, and d4 are invalid parameters, and their values are shown in Table 2.

4. Analysis of the Results of Numerical Calculations

The temperature change of the material during processing can be obtained after analysis using the finite element software ABAQUS. In this paper, The temperature cloud diagram of the processing process is used to analyze the temperature change during this process. The results are shown in Figures 4 and 5. It can be clearly seen from these two figures that the area where the temperature rises sharply is the area where the chips remain, that is, the valley area of the milling texture. In the peak area of the milling texture, the temperature of the blade surface element does not rise sharply. The reason for this phenomenon is as follows: on the one hand, because the simulation analysis is a single grinding, the microelements on the blade surface are not constantly rubbed, which causes the temperature of the system to rise and accumulate. On the other hand, the large amount of heat generated during grinding is mostly attached to the chip body. The grinding simulation setting defaults that the cut chips are completely separated from the workpiece, so there is a significant temperature increase in the area where the chips remain. The areas where there are no residual chips, that is, those areas where the chips have been evacuated, will not cause a sharp rise in the surface temperature of the blade. The heat generated by mechanical friction during processing is removed with the removal of chips. It can be seen that it is very necessary to remove chips in time.

This paper distinguishes two different simulations and experiments in which the blade is at rest and the blade is in motion, in order to maximize the accuracy of the calculation. Figures 6 and 7, respectively, show the constraints of these two simulations; due to the different constraint conditions, the former cannot be simply defined as the state where the speed of the latter is zero. The simulation calculation amount of the blade and the belt at the same time is several

Figure 9: Cooling air flow velocity in the contact area during blade machining.

Figure 10: Cooling air flow velocity in the space near the processing area.

times that of the static and fixed state of the blade. In addition, the geometric characteristics of the original shape of the blade surface in the collection and distribution model should be as close as possible to the real blade blank surface.

Except that the setting of abrasive material parameter G_m is controlled by empirical value, other detailed parameters setting can be carried out as described below:

The hardness parameter H of the abrasive particle group is controlled by changing the parameters of the material. Change the speed of the reference point rotation (load-boundary condition) by setting the speed values of the six degrees of freedom in the boundary conditions, thereby controlling the movement frequency f of the abrasive particle group. On this basis, the linear velocity vs. of the abrasive particle group is controlled by changing the radius of gyration of the abrasive particle group movement (that is, the distance between the reference point and the abrasive particle group). Similarly, this control method is also adopted for the motion parameter v_w of the blade surface model,

We can control the normal force Fn between the blade and the abrasive particle group by changing the MPC contact option parameter (interaction-MPC constraint) in the constraint options. The definition of MPC is multipoint constraints; that is, the constraint point is not a single contact form. The tangential force Ft between the blade and the group of abrasive particles is controlled by setting the interaction property-tangential behavior in the interaction property, and the number of revolutions N of the abrasive particle group in a period of time is controlled by setting the time step (step-time period). The cooling condition constant adopts the default preset value, that is, the reduced air flow rate (Kg/min) produced by the high-speed rotation of the grinding tool, so that the workpiece can be effectively cooled during processing.

Figure 8 shows a set of simulation results that meet the above settings. The results show that the machining results achieve the expected results under the cooling conditions of the air flow generated by the grinding tool. The cooling condition constant changes due to changes in various parameters of the tool, and the cooling effect brought about by this change is in line with the processing requirements.

5. Experiment and Analysis

According to the above calculation results, the airflow generated by the high-speed rotating grinding tool can meet the requirements of velocity and flow rate; meanwhile, the heat carried by the chips will not cause the local temperature of the blade surface to rise too high. This paper uses an air flow meter to measure the cooling air flow conditions in the actual process. Figures 9 and 10 show that when the machine rotates at a certain speed, the air velocity in the contact area of the blades and the contact wheel and the air velocity in the space near the processing area are, respectively, 7.413 m/s and 5.903 m/s, and the airflow temperature is about 15 degrees Celsius.

In an open situation, the total pressure ratio of the cooling airflow can be set to 1.1, the airflow temperature is 288 k, the atmospheric pressure is 0.101Mpa, and the air density is 1.2Kg/m3. At this time, the cooling airflow mass flow on the processing surface can be used as follows The formula shown approximates:

$$q_m = V\rho_0 \Pi. \tag{11}$$

In the above formula, q_m is the mass flow rate of the cooling gas, ρ_0 is the air density, and Π is the total pressure ratio of the airflow.

If the area of the air flow around the processing area is 0.01m^2, then the air flow rates of the two are 5.75Kg/min and 4.57Kg/min, respectively. In the simulation calculation, it can be considered that the cooling airflow generated by the rotation of the grinding tool is equivalent to the flow rate of 5kg/min. More powerful ventilation air flow and cooling effect need to be achieved by generating cooling airflow through an air compressor. Obviously, the cooling effect of the airflow is closely related to the geometry of the tool. The research in this article can give such a processing idea: it is possible to design a processing tool that can not only conform to the blade surface grinding, but also generate high-speed cooling airflow due to the movement of the tool itself. This tool will change the shape of the contact wheel of the belt machine. These work will be carried out in further research.

6. Summary and Outlook

On the basis of the plate heat transfer model, the characteristics of the cooling airflow during the blade surface processing are studied. The cooling coefficient of the airflow is affected by the speed and pressure. The generation and strength of the self-generating cooling airflow are closely related to the physical properties of the grinding tool. In terms of processing heat generation, this paper uses the Johnson-Cook material constitutive model to calculate the residual heat on the surface of the processed blade, and the surface temperature rise is within a controllable range.

For the airflow intensity generated by the high-speed rotation of the tool, the airflow preset method is used to verify whether it meets the processing conditions. In the subsequent research, in addition to the plate heat transfer model, the conical capillary model can also be used as the cooling airflow model. It is necessary to improve the shape of the processing tool so that it can not only meet the requirements of blade surface processing, but also generate high-speed cooling airflow. Future research can be combined with cooling and lubrication, air flow types, etc. to increase the breadth and depth of research.

Data Availability

The data that support the findings of this study are available from the corresponding author upon reasonable request.

Conflicts of Interest

The authors declared no potential conflicts of interest with respect to the research, authorship, and/or publication of this article.

Acknowledgments

This research was funded by the Ningbo University of Technology Research Startup Fund (No. ZX2020000395) and the Ningbo Science and Technology Innovation 2025 Major Special Project (No. 2020Z109).

References

[1] F. Klocke, S. L. Soo, B. Karpuschewski et al., "Abrasive machining of advanced aerospace alloys and composites," *Cirp Annals-manufacturing technology*, vol. 64, no. 2, pp. 581–604, 2015.

[2] G. A. Oosthuizen, *Innovative Cutting Materials For Finish Shoulder Milling Ti-6A1-4V Aero-Engine Alloys*, Stellenbosch University of Stellenbosch, Western Cape, 2009.

[3] Z. Chen, Y. Shi, X. Lin et al., "A profile-adaptive compliant polishing tool for aero-engine blade finishing process," *The International Journal of Advanced Manufacturing Technology*, vol. 102, no. 9-12, pp. 3825–3838, 2019.

[4] B. Denkena, V. Boess, D. Nespor, F. Floeter, and F. Rust, "Engine blade regeneration: a literature review on common technologies in terms of machining," *The International Journal of Advanced Manufacturing Technology*, vol. 81, no. 5-8, pp. 917–924, 2015.

[5] S. B. T. Raj, "Advanced material for front fan blade manufacturing," *Imperial Journal of Interdisciplinary Research*, vol. 3, no. 5, pp. 80–88, 2017.

[6] R. K. Vimal and G. Dhanjayan, "Improving fatigue life of gas turbine fan blade using advanced composite materials," *IOP Conference Series: Materials Science and Engineering*, vol. 455, no. 1, article 012035, 2018.

[7] N. S. Babu and K. J. Rao, "Strength assessment of fan blade with different materials," *Science and Technology*, vol. 6, no. 1, pp. 266–283, 2019.

[8] X. U. Xiaohu, Z. H. Dahu, H. Zhang, Y. A. Sijie, and D. I. Han, "Application of novel force control strategies to enhance robotic abrasive belt grinding quality of aero-engine blades," *ChineseJournal of Aeronautics*, vol. 32, no. 10, pp. 2368–2382, 2019.

[9] S. C. Xiu, Y. D. Gong, and G. Q. Cai, "Study on effect of grinding fluid supply parameters on surface integrity in quick-point grinding for green manufacturing," *Advanced Materials Research*, vol. 53-54, pp. 209–214, 2008.

[10] C. Mao, H. Zou, Y. Huang, Y. Li, and Z. Zhou, "Analysis of heat transfer coefficient on workpiece surface during minimum quantity lubricant grinding," *International Journal of Advanced Manufacturing Technology*, vol. 66, no. 1-4, pp. 363–370, 2013.

[11] H. Singh, V. S. Sharma, S. Singh, and M. Dogra, "Nanofluids assisted environmental friendly lubricating strategies for the surface grinding of titanium alloy: Ti6Al4V-ELI," *Journal of Manufacturing Processes*, vol. 39, no. MAR., pp. 241–249, 2019.